1.D.2 *Nuclear Physics* A323 (1979) 446–460;

MAGNETIC QUADRUPOLE RESONANCE IN SPHERICAL NUCLEI

V. Yu. PONOMAREV, V. G. SOLOVIEV, Ch. STOYANOV and A. I. VDOVIN
Joint Institute for Nuclear Research, Laboratory of Theoretical Physics, Dubna

Received 29 January 1979

Abstract: The distribution of the M2 strength in spherical nuclei is studied within the quasiparticle-phonon nuclear model. It is shown that the interaction of the one- and two-phonon states affects strongly this distribution at the excitation energies $E_x > 15$ MeV. In all the nuclei the strength of the M2 transitions is concentrated in the excitation energy region of 6–12 MeV. At these energies the calculated total value of $B(M2)\uparrow$ is in good agreement with the experimental data in ^{90}Zr and ^{208}Pb. The calculations show that a group of states observed in ^{58}Ni at an energy of about 7 MeV in the (e, e′) experiments is a part of the M2 resonance.

1. Introduction

In recent years a good deal of attention has been paid to the theoretical and experimental study of the giant resonances in medium and heavy atomic nuclei. The most important result of the experiments on the inelastic scattering of electrons at large angles is the discovery of the magnetic quadrupole resonance. The M2 resonance was first detected in ^{208}Pb in the Naval Research Laboratory, Washington (NRL) [1]. These data were verified in (e, e′) experiments with high resolution at the linear accelerator in Darmstadt, where the M2 resonance was also identified in ^{90}Zr [refs. [2–4])]. The concentration of the M2 strength in ^{90}Zr at an energy of $E_x \approx 9$ MeV was observed earlier [5]). We should like to mention the investigations performed on the Ni isotopes by the group in NRL. They contain indirect indications as to the existence of 2^- states at energies from 6 to 8.5 MeV in ^{58}Ni.

The M2 resonance in ^{90}Zr and ^{208}Pb was studied in several papers. The Jülich group [7,8]) have studied the influence of the 2p-2h configurations on the distribution of M2 strength within the finite Fermi-systems theory. The calculations in the RPA were performed also within the MSI model [2,3,9]) and for ^{208}Pb with effective separable spin-dipole forces [10]). It should be noted that in these calculations ^{90}Zr was considered as a doubly magic nucleus, i.e., the superconducting pairing forces in the proton system were not taken into account.

In this paper the M2 resonance is studied in ^{58}Ni, ^{90}Zr, ^{120}Sn, ^{140}Ce and ^{208}Pb within the quasiparticle-phonon model [11,12]). The most detailed calculations have been performed for ^{90}Zr and ^{58}Ni. A comparison is made with the available experimental data and with calculations of other authors.

2. Formulae and numerical details

The Hamiltonian in the quasiparticle-phonon nuclear model includes the average field for protons and neutrons, the pairing interaction and the effective long-range forces [12]). The effective long-range forces generate in a doubly even nucleus the phonon excitations with different angular moments and parities. The phonons with $I^\pi = 1^-, 2^+, \ldots 7^-$ are generated by the separable multipole forces, and the phonons with $I^\pi = 1^+, 2^-, 3^+, \ldots 6^-$ by the spin-multipole forces. Both the isoscalar and isovector parts of the effective forces have been taken into account. Thus the one-phonon states with $I^\pi = 2^-$ have been calculated in the RPA using separable spin-dipole forces,

$$\tfrac{1}{2}(\kappa_0^{(12)} + \kappa_1^{(12)}\tau_1 \cdot \tau_2) r_1 \cdot r_2 [\sigma_1 Y_{1\mu}(\theta_1\varphi_1)]_{2^-} \cdot [\sigma_2 Y_{1\mu}(\theta_2\varphi_2)]_{2^-}.$$

Besides the calculation in the RPA, we have performed the calculations taking into account the interaction of the one- and two-phonon states. The wave function of the 2^- state was taken in the form

$$\Psi_\nu(2^- M) = \{\sum_i R_\nu(2^- i) Q^+_{2Mi} + \sum_{\substack{\lambda_2\lambda_1 \\ i_2 i_1}} P^{\lambda_2 i_2}_{\lambda_1 i_1}(2^- \nu)[Q^+_{\lambda_1\mu_1 i_1} Q^+_{\lambda_2\mu_2 i_2}]_{2^- M}\}|0\rangle. \tag{1}$$

In (1) the following notation is used: $Q^+_{\lambda\mu i}$ is the phonon creation operator with angular momentum λ, projection μ and number i, and $|0\rangle$ is the wave function of the ground state of a doubly even nucleus (phonon vacuum $Q_{\lambda\mu i}|0\rangle = 0$). To find the energies and the structure of states described by the wave function (1), one should solve a very complicated system of nonlinear equations [12, 13]) of large dimension. As shown in ref. [12]), it is simplier to calculate the M2 transition strength function $b(\mathrm{M2}, \eta)$ which is determined as follows:

$$b(\mathrm{M2}, \eta) = \sum_\nu B(\mathrm{M2}, 0^+_{\mathrm{g.s.}} \to 2^-_\nu) \frac{\Delta}{2\pi} \frac{1}{(\eta - \eta_\nu)^2 + \frac{1}{4}\Delta^2}. \tag{2}$$

The reduced probability $B(\mathrm{M2}; 0^+_{\mathrm{g.s.}} \to 2^-_\nu)$ of excitation of the 2^-_ν state from the ground one is calculated by the formula

$$B(\mathrm{M2}, 0^+_{\mathrm{g.s.}} \to 2^-_\nu) = |\sum_i R_\nu(2^- i)\langle 0||\mathscr{M}(\mathrm{M2}) Q^+_{2\mu i}||0\rangle|^2. \tag{3}$$

Formula (3) for $B(\mathrm{M2}, 0^+ \to 2^-_\nu)$ is obtained under the assumption that the terms in the operator $\mathscr{M}(\mathrm{M2})$ which do not change the number of quasiparticles (i.e. $\sim \alpha^+\alpha$) give a negligible contribution to the probability of excitation of the 2^- states and therefore are not taken into account.

The average field is described by the Saxon-Woods potential, the parameters of which have been chosen according to ref. [14]). The single-particle energies and the radial part of the wave functions have been found by solving numerically the Schrödinger equation by the method suggested in ref. [15]). As a result, the single-particle spectra used in this paper differ from those obtained earlier [13]) by the semianalytic method of solving the Schrödinger equation [16]). The new spectra have a larger density of single-particle levels, and what is more essential, the quasibound state wave functions have the correct asymptotic behaviour. This made it possible to take into account the quasibound states with a relatively small width. The constants of the superconducting pairing interaction G_N and G_Z have been determined from the experimental values of the pairing energies. The parameters of the single-particle potential and the values of the constants $G_{N,Z}$ are given in table 1.

TABLE 1

The parameters of the Saxon-Woods potential and the pairing interaction constants

A		r_0 (fm)	V_0 (MeV)	κ (fm^2)	α (fm^{-1})	G_{NZ}
59	$N = 31$	1.31	46.2	0.413	1.613	0.280
	$Z = 27$	1.24	53.7	0.308	1.587	0.302
91	$N = 53$	1.29	44.7	0.413	1.613	0.168
	$Z = 39$	1.24	56.9	0.338	1.587	0.194
121	$N = 71$	1.28	43.2	0.413	1.613	0.122
	$Z = 51$	1.24	59.9	0.346	1.587	0.136
141	$N = 83$	1.27	46.0	0.413	1.613	0.116
	$Z = 59$	1.24	57.7	0.349	1.587	0.122
209	$N = 127$	1.26	44.83	0.376	1.587	0.074
	$Z = 83$	1.24	60.3	0.371	1.587	0.080

The constants of the effective long-range forces have mainly been determined from the experimental data. We also used the estimates of refs. [10,17]). The constants of dipole forces have been chosen so as to describe correctly the E1 resonance energy and satisfy the condition that the energy of the first 1^- state be zero in the RPA. The latter condition allows one to exclude with good accuracy the influence of the spurious state which is caused by the breaking of translational invariance [18]). The constants of the separable quadrupole and octupole interactions have been chosen so as to describe correctly the energies of the 2_1^+ and 3_1^- states taking into account the two-phonon admixtures [13,19]). The ratio of the isoscalar and isovector constants has been determined by the formula

$$q^{(\lambda)} = \kappa_1^{(\lambda)}/\kappa_0^{(\lambda)} = -0.2(2\lambda+3). \tag{4}$$

Formula (4) coincides with the estimates suggested by Bohr and Mottelson [17]) except for a numerical factor (see also ref. [20])). The different numerical factor

obtained for the oscillator single-particle potential [17]) overestimates the energies of the isovector E2 resonance in calculations with a Saxon-Woods potential. As is shown in refs. [13,21]), the correct position of the isovector E2 resonance is obtained in this case at $q^{(2)} = -(1.4\text{–}1.5)$. The constants of the multipole forces with $\lambda > 3$ are taken to be less by a factor of 1.2–1.5 than those of ref. [17]). The collective states with low energy and $I > 3$ do not appear at these values of the constants. For the separable spin-multipole forces, the values of the constants are as follows:

$$\kappa_0^{(\lambda L)} = 0, \qquad \kappa_1^{(\lambda L)} = -\frac{28 \times 4\pi}{A\langle r^\lambda \rangle^2} \text{ MeV} \cdot \text{fm}^{-2\lambda}. \tag{5}$$

The dependence on A and λ in these formula results from the qualitative considerations, and the numerical factor in the expression for $\kappa_1^{(\lambda L)}$ is chosen from the experimental energy of the M1 resonance in spherical nuclei [22]); it is close to the results of ref. [10]). Indeed, the constants (5) are not very accurate, but their change by a factor of 1.5–2 does not essentially change the final results. The dependence of the results on the constants $\kappa_0^{(12)}$ and $\kappa_1^{(12)}$ is discussed for the 2^- states in sect. 3. We have used the following values: $g_s^{\text{eff}} = 0.8\, g_s^{\text{free}}$, $g_l^{\text{n}} = 0.0$, $g_l^{\text{p}} = 1.0$ for the effective gyromagnetic factors. The constants thus chosen (including g_s, g_l-factors) have been used also for the calculation of the E1 and M1 resonances; good agreement with experiment has been obtained [13,23]). The parameter Δ used for the calculation of the strength function $b(\text{M2}, \eta)$ is taken to be equal to 0.1 MeV.

3. The M2 resonance in ^{90}Zr

First we shall discuss the results for ^{90}Zr. The distribution of the M2 strength calculated in the RPA for different values of the constants $\kappa_0^{(12)}$ and $\kappa_1^{(12)}$ is given in figs. 1a–1d. At the values of $\kappa_1^{(12)} \approx -(30\text{–}40)4\pi/A\langle r^2 \rangle$ the main M2 strength is concentrated in two regions: $E_x = 8\text{–}12$ MeV ($\sum B(\text{M2})\uparrow = 2900\ \mu^2 \cdot \text{fm}^2$ where μ_N is the nuclear magneton) and $E_x \approx 18\text{–}20$ MeV comprising a state with the maximal value of $B(\text{M2})\uparrow \approx 1600\text{–}1800\ \mu_N^2 \cdot \text{fm}^2$. This state is strongly collectivized. The change of the isoscalar constant $\kappa_0^{(12)}$ does not influence the distribution. Increasing $|\kappa_0^{(12)}|$ results in the concentration of M2 strength in individual states only, i.e., in a decrease in the number of the 2^- levels with a considerable value of $B(\text{M2})\uparrow$. The spin-dipole effective n-p forces are so weak at $\kappa_0^{(12)} = 0.9\ \kappa_1^{(12)}$ that the one-phonon states consist either of neutron or proton two-quasiparticle components only. With decreasing $|\kappa_1^{(12)}|$ the aforesaid regions of strong M2 transitions approach each other and the M2 strength concentrates at $E_x \approx 10$ MeV. The strongest 2^- state becomes less collective and its energy and value of $B(\text{M2})$ decrease. It should be noted that all the 2^- states with large values of $B(\text{M2})$ correspond to the transitions over one shell.

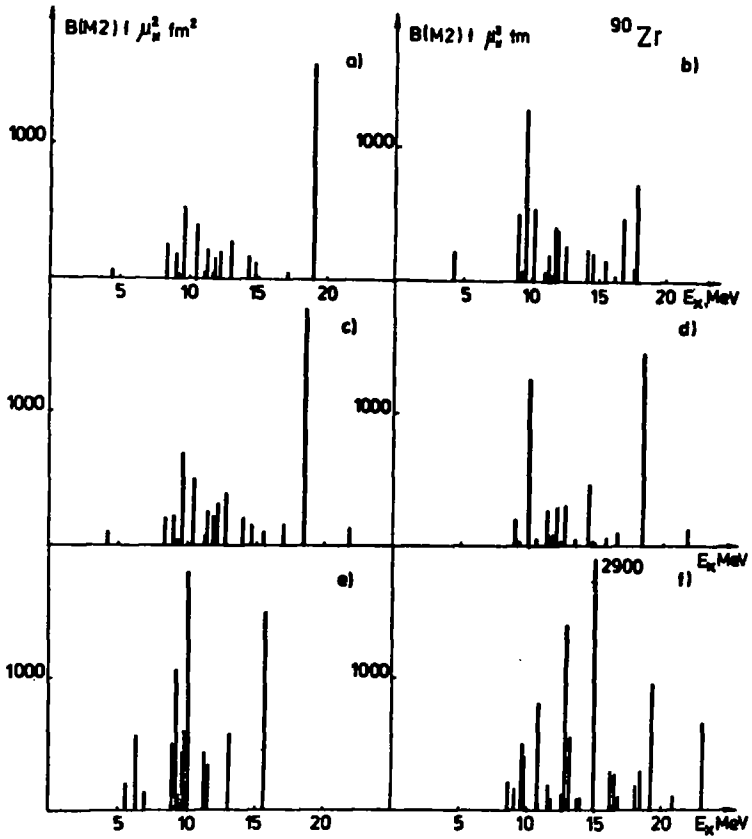

Fig. 1. Magnetic quadrupole resonance in ^{90}Zr. Calculations in the RPA: (a) $\kappa_0^{(12)} = 0$, $\kappa_1^{(12)} = -37 \times 4\pi/A\langle r\rangle^2$ MeV · fm^{-2}. (b) $\kappa_0^{(12)} = 0$, $\kappa_1^{(12)} = -14 \times 4\pi/A\langle r\rangle^2$ MeV · fm^{-2}. (c) $\kappa_0^{(12)} = 0$, $\kappa_1^{(12)} = -28 \times 4\pi/A\langle r\rangle^2$ MeV · fm^{-2}. (d) $\kappa_0^{(12)} = 0.9\kappa_1^{(12)}$, $\kappa_1^{(12)} = -28 \times 4\pi/A\langle r\rangle^2$ MeV · fm^{-2}. (e) Calculation within the MSI model [3]). The gyromagnetic factors are free. (f) Calculation within the theory of finite Fermi systems [8]). The gyromagnetic factors are free.

Table 2 shows the experimental and theoretical data of various authors on the total M2 transition probability in ^{90}Zr in the interval ΔE_x = 8–10 MeV:

$$B_\Sigma(\mathrm{M2}) = \sum_{i \in \Delta E_x} B(\mathrm{M2}, 0^+_{\mathrm{g.s.}} \to 2^-_i).$$

These data show that with the constants (5) the theoretical results in the RPA are in good agreement with experiment. The change of the constants $\kappa_0^{(12)}$ and $\kappa_1^{(12)}$ within reasonable limits results in the change of B_Σ(M2) by a factor of 1.5–2.0. Our results for B_Σ(M2) are close to the results of calculations within the theory of finite Fermi systems with free values of the gyromagnetic factors [8]). But the general picture of the distribution of M2 strength in the excitation energy region 0–25 MeV is more close to the calculations by the MSI model [3]) (fig. 1e). The comparison of

TABLE 2

Experimental and theoretical values of $\sum_{i\in\Delta E_x} B(\mathrm{M2}, 0^+ \to 2_i^-)\mu_N^2 \cdot \mathrm{fm}^2$ for ΔE_x = 8–10 MeV in ^{90}Zr and ΔE_x = 6.1–8.4 MeV in ^{208}Pb

Nuclei	Exp. refs. [2,3])	Present results						MSI model refs. [2,3]) 1p-1h	Ref. [10]) 1p-1h	Theory of finite Fermi systems. Effective (free) M2 operator ref. [8])	
		$\kappa_0^{(12)} = 0$, $\kappa_1^{(12)} = -\frac{28\times 4\pi}{A\langle r\rangle^2}$		$\kappa_0^{(12)} = 0$, $\kappa_1^{(12)} = -\frac{14\times 4\pi}{A\langle r\rangle^2}$		$\kappa_0^{(12)} = 0.9\kappa_1^{(12)}$, $\kappa_1^{(12)} = -\frac{28\times 4\pi}{A\langle r\rangle^2}$				1p-1h	1p-1h + 2p-2h
		RPA	$Q^+ + Q^+Q^+$	RPA	$Q^+ + Q^+Q^+$	RPA	$Q^+ + Q^+Q^+$				
^{90}Zr	1100±100	1090	1100	1900	2100	1420	1000	4500		640(1280)	(1190)
^{208}Pb	8500±750	9700		12600		9850		13000	11000	11600	9100

$\kappa_0^{(12)}$ and $\kappa_1^{(12)}$ are in MeV · fm^{-2}

figs. 1b and 1e shows that the results obtained in ref. [3]) are very close to ours at $\kappa_1^{(12)} \approx -10 \times 4\pi/A \langle r \rangle^2$ MeV · fm^{-2}. Here we can separate two regions which concentrate strong M2 transitions, the maximum of B(M2) being at an energy of $E_x \approx 10$ MeV. The distribution of the M2 strength calculated within the theory of finite Fermi systems in the RPA is of quite a different form (fig. 1f). The strong M2 transitions appear in a wide energy region from 8 to 20 MeV, and the maximum of B(M2) is at an energy of $E_x = 15$ MeV. As shown in ref. [8]) the main features of the distribution are slightly sensitive to the parameters of the residual forces (see

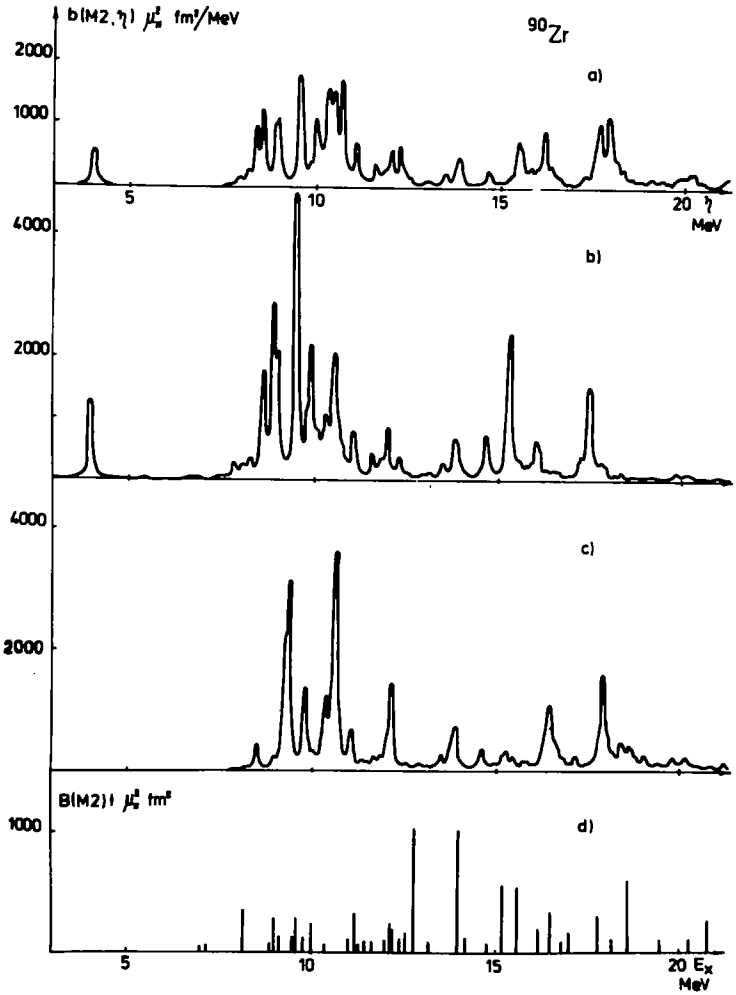

Fig. 2. The M2 resonance in ^{90}Zr taking into account the one- and two-phonon states: (a) $\kappa_0^{(12)} = 0$, $\kappa_1^{(12)} = -28 \times 4\pi/A\langle r \rangle^2$ MeV · fm^{-2}. (b) $\kappa_0^{(12)} = 0$, $\kappa_1^{(12)} = -14 \times 4\pi/A\langle r \rangle^2$ MeV · fm^{-2}. (c) $\kappa_0^{(12)} = 0.9$ $\kappa_1^{(12)}$, $\kappa_1^{(12)} = -28 \times 4\pi/A\langle r \rangle^2$ MeV · fm^{-2}. (d) Calculation within the theory of finite Fermi systems taking into account the mixing of 1p-1h and 2p-2h configurations [8]).

fig. 36 of ref. [8])). The difference between the predictions of this paper and ref. [8]). is caused mainly by different single-particle schemes. The single-particle neutron and proton schemes for ^{90}Zr given in ref. [8]) differ from our schemes by a much lesser density of hole levels and a smaller distance between the unfilled and neighbouring major shells. We have performed the calculation of the M2 resonance in ^{90}Zr using the single-particle schemes of ref. [8]) and our effective forces. The result is rather close to that in figs. 1f. This means that the concrete form of the effective forces is of no importance.

The interaction of the one- and two-phonon states changes strongly the distribution of the M2 strength, especially at high excitation energies. The strength function $b(\mathrm{M2}, \eta)$ calculated at different values of the constants $\kappa_0^{(12)}$ and $\kappa_1^{(12)}$ is shown in figs. 2a–2c. In these calculations the one-phonon part of the wave function (1) included 14 one-phonon 2^- states with the largest values of $B(\mathrm{M2})$ in the excitation energy interval 0–25 MeV. These 14 states exhaust 90 % of the total M2 strength in this interval. The two-phonon part of the wave function included more than 800 states for which the matrix element of the interaction with the one-phonon states was not less than 3 % of its maximal value. The lower group of strong M2 transitions is slightly affected by the two-phonon admixtures. It almost conserves its position, the width of location and the total strength of the M2 transitions. The $B_\Sigma(\mathrm{M2})$ value changes slightly too. From table 2 one can see that the $B_\Sigma(\mathrm{M2})$ values calculated both in the RPA and taking into account the interaction of the one- and two-phonon states are in satisfactory agreement with experimental data. Strong changes occur in the collective state at $E_x \approx 18$ MeV. Its interaction with the two-phonon states causes an almost complete spreading of the high-lying branch of the M2 resonance. Table 3 gives the M2 strength distribution in the spectrum of ^{90}Zr obtained both in the RPA and taking into account the interaction of one- and two-phonon states (the constants $\kappa_0^{(12)}$ and $\kappa_1^{(12)}$ correspond to eq. (5)). It is seen

TABLE 3

M2 strength distribution in ^{90}Zr and ^{58}Ni calculated in RPA and taking into account the interaction of one- and two-phonon states

Nuclei	ΔE (MeV)	0–6	6–8	8–10	10–12	12–14	14–16	16–18	18–20	20–25
^{90}Zr	$\sum_{\Delta E} B(\mathrm{M2})\uparrow(\mu_N^2 \cdot \mathrm{fm}^2)$ RPA	90		1090	930	640	430	130	1800	
	$\int_{\Delta E} \frac{b(\mathrm{M2}, \eta)\mathrm{d}\eta}{(\mu_N^2 \cdot \mathrm{fm}^2)}$	100	54	1100	1300	400	440	790	410	300
^{58}Ni	$\sum_{\Delta E} B(\mathrm{M2})\uparrow(\mu_N^2 \cdot \mathrm{fm}^2)$ RPA			440	930	220	220	240		1200
	$\int_{\Delta E} \frac{b(\mathrm{M2}, \eta)\mathrm{d}\eta}{(\mu_N^2 \cdot \mathrm{fm}^2)}$		590	530	300	250	370	300	110	450

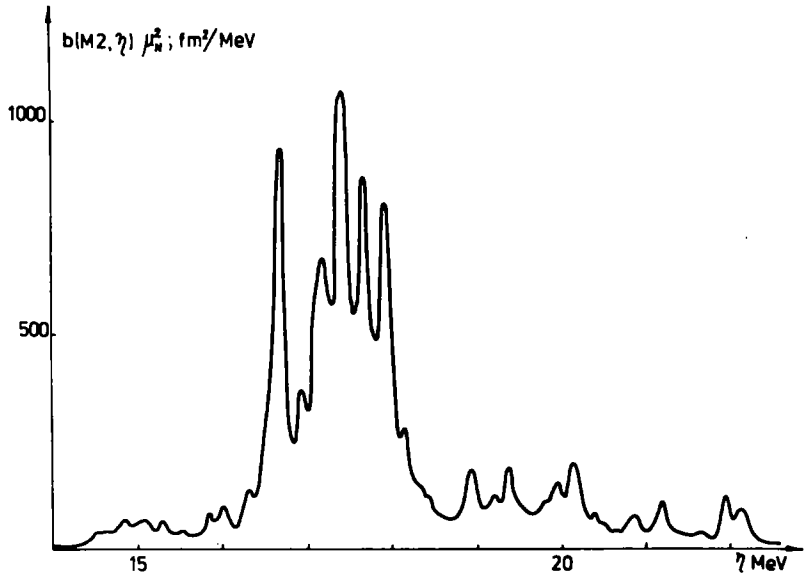

Fig. 3. The strength distribution of the one-phonon state with $E_x = 18$ MeV. For the constants see fig. 1c).

that the M2 strength corresponding to the strong 2^- state at $E_x = 18$ MeV is spread in an interval of about 10 MeV. Fig. 3 shows the strength function describing the fragmentation of this state only (without allowing for the influence of other one-phonon 2^- states). Fig. 3 clearly demonstrates the appearance of the width of an "infinitely narrow" resonance due to the interaction with more complex configura-tions. The reason for the strong fragmentation of the high-lying branch of the M2 resonance is the high collectivity of this state, resulting in a strong coupling with the two-phonon states, and in a large density of the two-phonon states at the excitation energies $E_x = 18$ MeV. To what extent this result is stable to changes in the constants of the effective spin-dipole forces, can be seen from figs. 2a, 2b and 2c. The absence of the strong concentration of the M2 strength at large excitation energies is a common feature of these pictures. At $\kappa_1^{(12)} \approx -10 \times 4\pi/A \langle r \rangle^2$ MeV $\cdot$ fm^{-2} the collective state with $E_x = 18$ MeV is absent already in the RPA; at larger values of $|\kappa_1^{12}|$ it spreads over the two-phonon states. The distributions of the M2 strength shown in figs. 2a–2c are much closer to each other than those calculated in the RPA. So, the essential concentration of the M2 strength is in the interval $E_x = 8$–12 MeV which comprises 45 % of the total value of B(M2) in the interval 0–25 MeV.

The influence of the interaction with complex configurations on the M2 resonance in ^{90}Zr has been studied also in the theory of finite Fermi systems [8]). The results of the corresponding calculations are given in fig. 2d (see also fig. 36 ref. [8])). As seen from figs. 1f and 2d, the interaction of 1p–1h and 2p–2h configurations results in a noticeable fragmentation of the M2 strength, but the main features of the distri-

bution are not changed. Table 2 shows also that the value of B_Σ(M2) in these calculations is slightly changed as well as in our calculations.

It has already been mentioned that the set of parameters used in our paper allows one to describe satisfactorily the available experimental data on the M1 resonance in spherical nuclei [23]). Fig. 4 shows the M1 resonance in ^{90}Zr calculated both in the

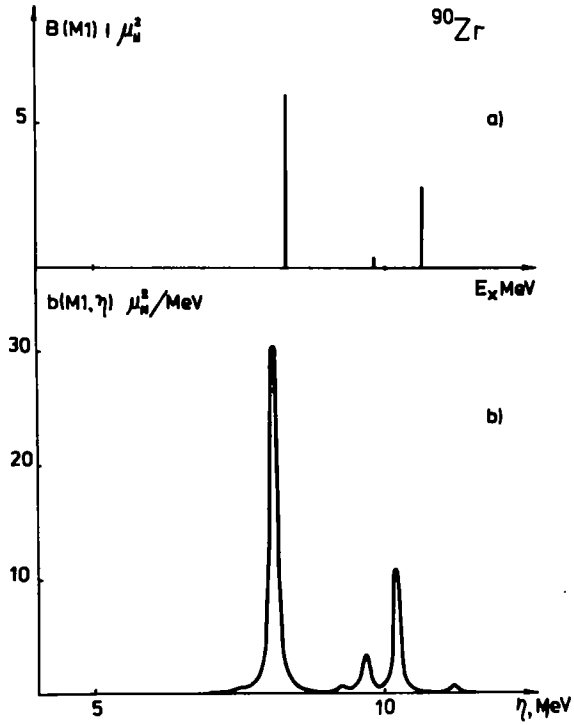

Fig. 4. The M1 resonance in ^{90}Zr: (a) Calculation in the RPA. (b) The strength function b(M1, η) taking into account the interaction of the one- and two-phonon states. The constants: $\kappa_0 = 0$, $\kappa_1 = -28 \times 4\pi/A$ MeV.

RPA (fig. 4a) and taking into account the interaction of the one- and two-phonon states (fig. 4b). The two-phonon admixtures do not influence strongly the M1 resonance, and therefore the main strength of the M1 transitions is concentrated in a narrow region around $E_x = 8$ MeV. The M1 and M2 resonances in ^{90}Zr are overlapped, and the total photoabsorption cross section for the M1 resonance is larger by the order of two than for the M2 resonance.

4. The M2 resonance in ^{58}Ni

The distribution of the M2 strength in ^{58}Ni calculated in the RPA has the same specific features as in ^{90}Zr (fig. 5a). In ^{58}Ni the regions of the strong M2

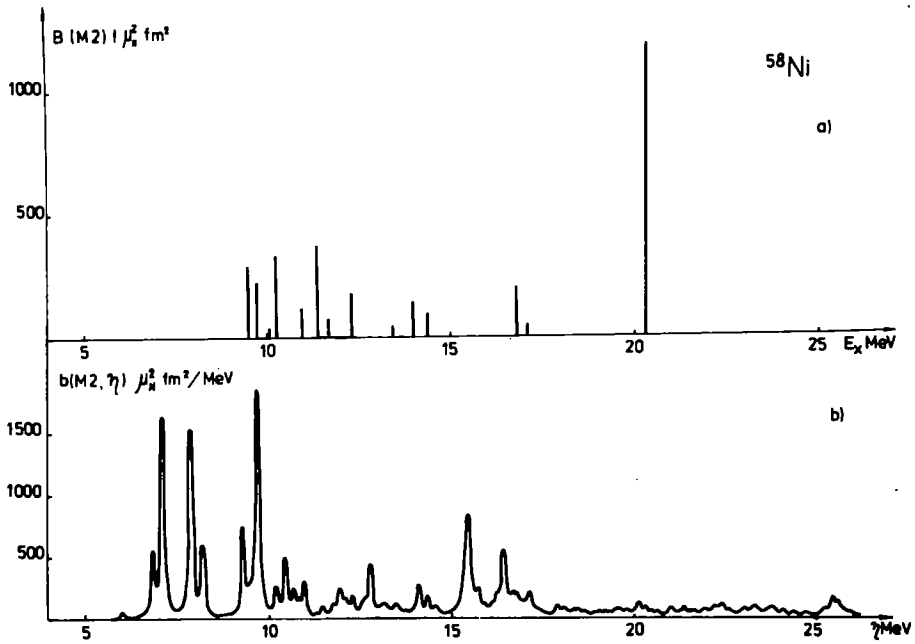

Fig. 5. The M2 resonance in ^{58}Ni: (a) Calculation in the RPA. (b) The strength function b(M2, η) taking into account the interaction of the one- and two-phonon states. The constants: $\kappa_0^{(12)} = 0$, $\kappa_1^{(12)} = -28 \times 4\pi/A\langle r\rangle^2$ MeV · fm^{-2}.

transitions lie at somewhat larger excitation energies: $E_x = 9.5$–12.5 MeV ($\sum$B(M2)↑ = 1570 $\mu_N^2 \cdot$ fm^2) and $E_x = 20$ MeV ($\sum B$(M2)↑ $\approx$ 1200 $\mu_N^2 \cdot$ fm^2). The interaction of the one- and two-phonon states changes this distribution considerably (fig. 5b). First, as in ^{90}Zr, the high-lying collective state strongly spreads. It is fragmented even more since at the excitation energy of 18–22 MeV in ^{58}Ni there is a group of two-phonon states to which it is coupled very strongly. Second, the group of the M2 transitions lying at an energy of 9.5–12.5 in the RPA lowers greatly and its mean energy is around 7 MeV. The data on the distribution of the M2 strength obtained both in the RPA and taking into account the interaction of the one- and two-phonon states are given in table 3. A considerable concentration of M2 strength at an energy of $E_x \approx 7$ MeV forces us to apply the results of the (e, e′) experiments [6]). As already mentioned in the introduction, a group of states was observed at an energy of 6–8 MeV in ^{58}Ni, which could not be established to consist either of the 1^+ or 2^- states. The theoretically calculated M1 transitions at this energy [23]) are not in agreement with the experimental B(M1)↑ (see fig. 6), though for the group of 1^+ states at 10–11 MeV calculations are in good agreement with experiment. According to the estimates of ref. [6]), if the states at 6–8 MeV have $I^\pi = 2^-$ then $\sum B$(M2)↑ $\approx$ 500 $\mu_N^2 \cdot$ fm^2. The total value of B(M2)↑ in this interval in our calculation is 700 $\mu_N^2 \cdot$ fm^2; this is in agreement with experiment. Thus, our

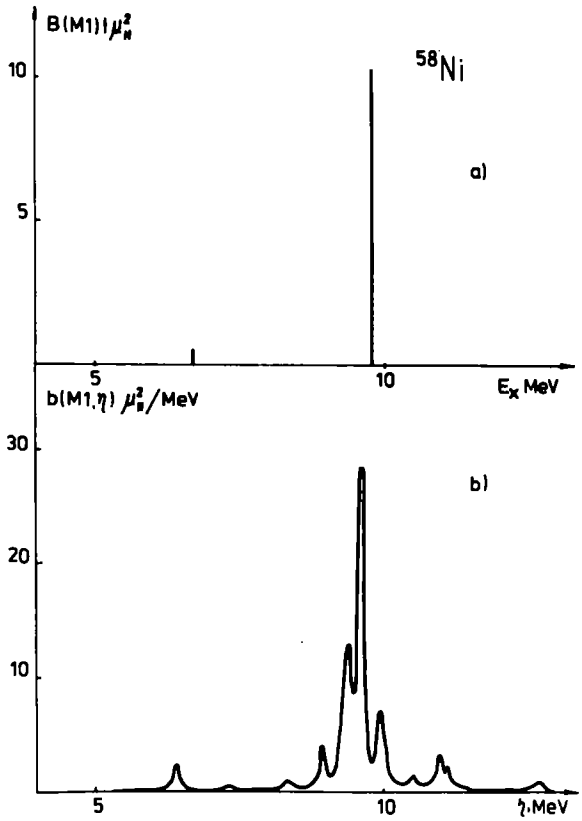

Fig. 6. The M1 resonance in ^{58}Ni: (a) Calculation in the RPA. (b) The strength function b(M1, η) taking into account the interaction of the one- and two-phonon states. The constants: $\kappa_0 = 0$, $\kappa_1 = -28 \times 4\pi/A$ MeV.

results testify to the assumption that a group of states observed in ^{58}Ni at 6–8 MeV [ref. [6])] consists mainly of 2^- states. It should be emphasized that this result is a consequence of the interaction of one- and two-phonon states.

5. The M2 resonance in the nuclei with $A > 100$

In this section we shall briefly discuss the predictions of the quasiparticle-phonon nuclear model for the M2 resonance in heavier nuclei. The distribution of the M2 strength in the interval E_x = 0–20 MeV in ^{120}Sn, ^{140}Ce and ^{208}Pb is given in fig. 7. The calculation has been performed in the RPA with the values of the constants (5). Though the main features of these distributions are almost the same as in ^{90}Zr and ^{58}Ni, certain differences should be mentioned. The nuclei with $A > 100$ have one region of strong M2 transitions with width of about 10 MeV bounded by the states with the largest value of B(M2) instead of two regions in ^{90}Zr and ^{58}Ni. The mean

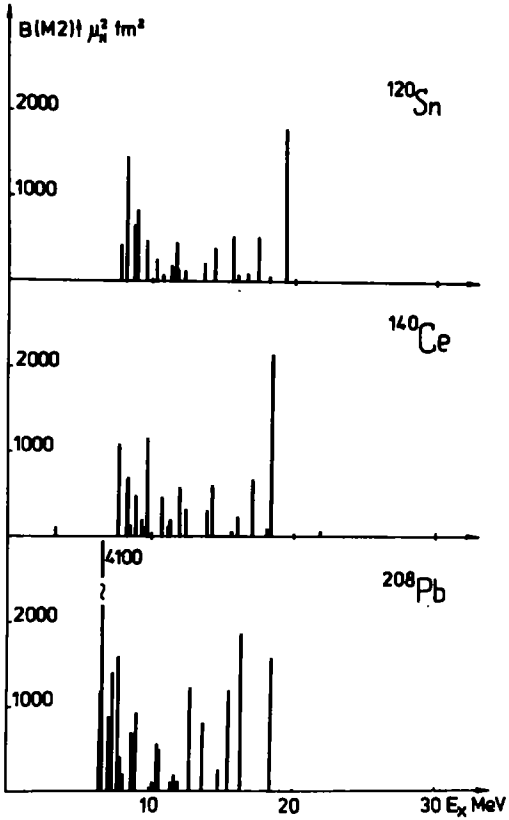

Fig. 7. The M2 resonance in ^{120}Sn, ^{140}Ce and ^{208}Pb. Calculation in the RPA. The constants: $\kappa_0^{(12)} = 0$, $\kappa_1^{(12)} = -28 \times 4\pi/A\langle r\rangle^2$ MeV · fm^{-2}.

energy of the region is lowered with increasing A. The results of calculations for ^{90}Zr and ^{58}Ni give evidence for the strong fragmentation of states at the energies $E_x > 15$ MeV.

Indeed, the calculation of the strength function b(M2, η) in ^{120}Sn shows that in

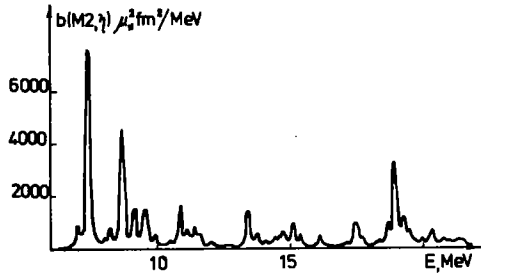

Fig. 8. The strength function b(M2, η) in ^{120}Sn calculated taking into account the interaction of the one- and two-phonon states. The constants: $\kappa_0^{(12)} = 0$, $\kappa_1^{(12)} = -28 \times 4\pi/A\langle r\rangle^2$ MeV · fm^{-2}.

this nucleus the M2 strength at the energies $E_x > 15$ MeV is distributed in a wide interval ΔE_x; its considerable concentration is observed only at $E_x \approx 7$–10 MeV (fig. 8). Note that due to computational difficulties, $b(\mathrm{M2}, \eta)$ in ^{120}Sn has been calculated with a very limited set of two-phonon states. Nevertheless, we think that this limitation only weakens the fragmentation of the one-phonon states.

Thus, our calculations show that a noticeable concentration of the M2 strength is observed in all spherical nuclei with $60 < A < 210$ at the energies $E_x \approx 6$–12 MeV. The quasiparticle-phonon model describes satisfactorily the total strength of the M2 transitions in this energy region. This is confirmed once more by the comparison of the experimental data and our results for ^{208}Pb (see table 2 which shows the data obtained by other authors too). Another important feature of our calculation is the absence of regions with a strong concentration of the M2 strength at $E_x > 12$ MeV.

6. Conclusion

Based on the results of this paper we can make two conclusions. First, this paper together with refs. [13,23]) shows that within the quasiparticle-phonon model with a unique set of parameters, one can describe satisfactorily a large portion of the experimental data on the Eλ, M1 and M2 resonances and radiative widths of the neutron resonances in spherical doubly even nuclei. We would like to note that at the same time the quasiparticle-phonon model describes well the low-lying nuclear excitations. On the other hand, our calculations show that all spherical nuclei concentrate an essential part of the total M2 strength at the excitation energies from 6–10 MeV. At higher excitation energies the regions with such a strong concentration of the M2 strength are absent. Note, that the regions of existence of the M1 and M2 resonances overlap, thus making it difficult to identify them.

The authors are grateful to V.V. Voronov, L. A. Malov and R. A. Eramzhyan for their continued interest in this paper and discussions.

References

1) R. A. Lindgren *et al.*, Phys. Rev. Lett. **35** (1975) 1423
2) R. Frey *et al.*, Phys. Lett. **74B** (1978) 45
3) W. Knüpfer *et al.*, Phys. Lett. **77B** (1978) 367
4) A. Richter, Proc. Sendai Conf. on electro- and photoexcitations, ed. Y. Kawazoe (Supp. Research Rep., Lab. Nucl. Science, Tohoku Univ., Tomizawa, Sendai, Japan 1977) p. 195
5) Y. Torizuka, Invited talk presented at the Colloque Franco-Japonais sur spectroscopie nucléaire et reaction nucléaire, Dogashima, Japan, 1976
6) R. A. Lindgren *et al.*, Phys. Rev. **C14** (1976) 1789
7) S. Krewald and J. Speth, Phys. Lett. **52B** (1974) 295
8) J. S. Dehesa, Ph.D. thesis, Rheinischen Friedrich-Wilhelms-Universitat zu Bonn, 1977
9) W. Knüpfer and M. G. Huber, Phys. Rev. **C14** (1976) 2254
10) B. Castel and I. Hamamoto, Phys. Lett. **65B** (1976) 27
11) V. G. Soloviev, Theory of complex nuclei (Pergamonn Press, Oxford, 1976)

12) V. G. Soloviev, JINR, E4-11012, Dubna, 1977; Particles and Nuclei **9** (1978) 810
13) V. G. Soloviev, Ch. Stoyanov and A. I. Vdovin, Nucl. Phys. **A288** (1977) 376;
V. G. Soloviev, Ch. Stoyanov and V. V. Voronov, Nucl. Phys. **A304** (1978) 503
14) V. A. Chepurnov, Yad. Fiz. **6** (1967) 955;
K. Takeuchi and P. A. Moldauer, Phys. Lett. **28B** (1969) 384
15) J. Bang *et al.*, Nucl. Phys. **A261** (1976) 59;
M. Kh. Gizzatkulov *et al.*, JINR, P11-10029, 1976, Dubna
16) N. Ju. Shirikova, JINR, P4-3712, Dubna, 1968
17) A. Bohr and B. Mottelson, Nuclear structure, vol. 2 (Benjamin, New York, 1974)
18) D. F. Petersen and C. J. Veje, Phys. Lett. **24B** (1967) 449;
N. I. Pyatov and D. I. Salamov, Nucleonika **22** (1977) 127
19) A. I. Vdovin and Ch. Stoyanov, Izv. Akad. Nauk SSSR (ser. fiz.) **38** (1974) 2604
20) D. R. Bès, R. A. Broglia and B. S. Nilsson, Phys. Reports **16C** (1975) 1
21) G. Kyrchev, L. A. Malov, V. O. Nesterenko and V. G. Soloviev, Yad. Fiz. **25** (1977) 951; JINR, E4-9962, Dubna, 1976
22) A. I. Vdovin, Ch. Stoyanov and I. P. Yudin, JINR, P4-11081, Dubna, 1977
23) V. Ju. Ponomarev, Ch. Stoyanov, A. I. Vdovin and V. V. Voronov, JINR, E4-12093, 1978, Dubna